

GIFT: Reconciling Post-Training Objectives via Finite-Temperature Gibbs Initialization

Zhengyang Zhao^{1,*}, Lu Ma^{1,*}, Yizhen Jiang^{1,2}, Xiaochen Ma¹, Zimo Meng¹,
Chengyu Shen¹, Lexiang Tang¹, Haoze Sun², Peng Pei², Wentao Zhang^{1,†}

¹Peking University ²Meituan

zhengyangzhao25@stu.pku.edu.cn, maluqaq@163.com

Abstract

The prevailing post-training paradigm for Large Reasoning Models (LRMs)—Supervised Fine-Tuning (SFT) followed by Reinforcement Learning (RL)—suffers from an intrinsic optimization mismatch: the rigid supervision inherent in SFT induces distributional collapse, thereby exhausting the exploration space necessary for subsequent RL. In this paper, we reformulate SFT to reconcile post-training objectives and propose Gibbs Initialization with Finite Temperature (GIFT). We characterize standard SFT as a degenerate zero-temperature limit that suppresses base priors. Conversely, GIFT incorporates supervision as a finite-temperature energy potential, establishing a distributional bridge that promotes objective consistency throughout the post-training pipeline. Our experiments demonstrate that GIFT significantly outperforms standard SFT and other competitive baselines when utilized for RL initialization, providing a mathematically principled pathway to preserve exploration and align the two post-training stages. Our code is available at <https://github.com/zzy1127/GIFT>.

1 Introduction

The training pipeline for Large Reasoning Models (LRMs) has converged into a standard two-stage paradigm. First, Supervised Fine-Tuning (SFT) establishes fundamental reasoning capabilities by leveraging expert demonstrations (Chung et al., 2022; Ouyang et al., 2022; Touvron et al., 2023). Second, Reinforcement Learning (RL) encourages the model to explore self-generated reasoning paths, allowing it to optimize for correctness beyond the constraints of static datasets (Shao et al., 2024a; Yu et al., 2025; Rafailov et al., 2024; Schulman et al., 2017). This hierarchical approach underpins current state-of-the-art reasoning sys-

tems (DeepSeek-AI et al., 2025b; Yang et al., 2025; Nvidia et al., 2024; Huang et al., 2026).

However, a fundamental theoretical discrepancy persists between these two phases. While SFT typically minimizes cross-entropy loss to imitate expert tokens, RL maximizes expected rewards through environmental exploration. Standard SFT aggressively suppresses the probability mass of non-target tokens, thereby forcing the policy distribution to collapse onto deterministic data points (Wu et al., 2025). This phenomenon, characterized as distributional collapse, erodes the structural priors inherited from pre-training and severely restricts the subsequent exploration space (Li et al., 2025). Consequently, as the model transitions to the RL stage, it encounters a critical bottleneck: the stochastic diversity required to discover high-reward trajectories has been effectively extinguished by the rigid supervision of the preceding SFT phase (Gudiband et al., 2023; Kang et al., 2025).

Previous research has attempted to mitigate this issue by heuristically tuning data mixtures and inter-stage scheduling (Kang et al., 2025; Liu et al., 2025b), or by modifying the SFT objective to implicitly incorporate RL properties (Zhu et al., 2025b; Wu et al., 2025; Du et al., 2025; Rafailov et al., 2024). In contrast to these methods, we do not attempt to bypass the RL stage or rely on heuristic adjustments; instead, we aim to establish a mathematically principled coupling between the two phases. We posit that SFT should not be treated as an isolated imitation task but rather as a rigorously defined initialization for subsequent RL within a unified global post-training framework.

Based on this insight, we derive a principled initialization for subsequent RL to reconcile post-training objectives, and propose **Gibbs Initialization with Finite Temperature (GIFT)** to realize this. GIFT ensures that while the model is trained to prioritize expert trajectories, it preserves the structural knowledge and inherent ca-

*Equal contribution.

†Corresponding author.

pabilities of the base model, offering a thermodynamic resolution to the alignment-exploration trade-off. Within our principled framework, standard SFT is characterized as a degenerate zero-temperature limit that induces a rigid distributional collapse onto the expert data. In contrast, GIFT maintains a finite temperature, enabling the model to incorporate expert supervision as a continuous re-weighting of the base distribution rather than a destructive overwrite.

Empirically, we conduct SFT followed by RL on a subset of the DeepMath-103k dataset (He et al., 2025). Experimental results demonstrate that GIFT significantly outperforms standard SFT and other robust SFT variants when utilized as an initialization policy for RL across diverse mathematical reasoning benchmarks and out-of-distribution (OOD) tasks. Furthermore, our geometric and distributional analyses reveal that GIFT maintains objective consistency throughout the two-stage post-training process. By preserving the exploration landscape, GIFT facilitates accelerated convergence and superior asymptotic performance during the subsequent RL stage, enhancing the model’s reasoning capabilities.

The contributions of this work are twofold, spanning theoretical and practical dimensions. Theoretically, by leveraging the well-established Gibbs optimal policy from KL-regularized RL, we provide a novel reinterpretation of the post-training pipeline. Specifically, we demonstrate that standard SFT acts as a degenerate zero-temperature limit of this theoretical optimum, directly causing distributional collapse. Practically, we propose GIFT to realize a principled finite-temperature initialization. Extensive experiments demonstrate that GIFT significantly outperforms robust SFT baselines on reasoning and OOD benchmarks, while maintaining superior objective consistency throughout the two-stage post-training pipeline.

2 Related Work

Post-training for Reasoning: SFT-then-RL Paradigm. Post-training for reasoning LLMs typically follows a two-stage paradigm: Supervised Fine-Tuning (SFT) and Reinforcement Learning with Verifiable Rewards (RLVR) (DeepSeek-AI et al., 2025a; Team et al., 2025; Liu et al., 2025b). SFT acts as a "cold-start" phase, establishing a strong initial policy by training on high-quality reasoning chains. Subsequently, RLVR enhances

problem-solving capabilities by allowing the model to explore the solution space beyond the SFT data, discovering novel and more robust reasoning paths. However, this transition is impeded by an intrinsic optimization conflict (Ouyang et al., 2022; Touvron et al., 2023). Specifically, SFT typically compels the model to fit deterministic one-hot labels, which aggressively suppresses the probability mass of alternative tokens. In contrast, RL necessitates a high-entropy policy distribution to facilitate exploration and the discovery of high-reward trajectories (Chen et al., 2025a; Zhang et al., 2024; Kumar et al., 2022; Niu et al., 2026). This mismatch often causes SFT to overfit specific patterns and induce a collapse of the probability manifold, thereby stifling the exploration capacity required for the subsequent RL stage (Kang et al., 2025; Vattikonda et al., 2025; Chen et al., 2025c).

Refining SFT and Bridging Post-Training Stages. To mitigate the distributional degradation inherent in standard SFT, numerous studies have refined its objective by modifying the training loss (e.g., dynamic re-weighting and clipping (Li et al., 2025; Wu et al., 2025; Zhu et al., 2025a,b)) or isolating loss calculations to critical high-entropy reasoning tokens (Wang et al., 2025; Jiang et al., 2025; Ruan et al., 2025). However, treating SFT as an isolated task often fails to address its overarching optimization mismatch with subsequent RL. To bridge this gap, alternative efforts seek to interleave the two stages (Ma et al., 2025; Zhang et al., 2025) or unify their objectives into a single framework (Yan et al., 2025; Ming et al., 2025; Liu et al., 2025a; Chen et al., 2025b). Despite their theoretical potential, these unified approaches introduce substantial computational complexity and have yet to supersede the empirically robust SFT-then-RL pipeline. In contrast, GIFT operates within this standard paradigm, proposing a lightweight, single-pass and mathematical principled initialization method designed to reconcile optimization objectives across the entire post-training process.

3 Method

In this section, we propose a novel training approach termed **Gibbs Initialization with Finite Temperature (GIFT)**. GIFT is grounded in the theoretical framework of reconciling the objectives of the two-stage post-training process, SFT and RL. Guided by the well-established Gibbs policy from KL-regularized RL, we derive a principled

initialization: a Gibbs distribution that serves as a theoretically motivated starting point for subsequent RL. Finally, we present an implementation that transforms this theoretical objective into a practical method for LLM training.

3.1 Preliminaries

Supervised Fine-Tuning. Starting with a pre-trained base model π_{base} and a curated dataset of high-quality demonstrations $\mathcal{D} = \{(x, y^*)\}$, SFT optimizes the model parameters θ to maximize the log-likelihood of the target sequences. The objective is typically formulated as a cross-entropy loss:

$$\begin{aligned} \mathcal{L}_{\text{SFT}}(\theta) &= -\mathbb{E}_{(x, y^*) \sim \mathcal{D}} \log \pi_{\theta}(y^* | x) \\ &= -\mathbb{E}_{(x, y^*) \sim \mathcal{D}} \sum_{t=1}^{|y^*|} [\log \pi_{\theta}(y_t^* | x, y_{<t}^*)]. \end{aligned} \quad (1)$$

By minimizing this negative log-likelihood, the model learns to imitate the distribution of the expert data, providing a specialized foundation for subsequent alignment or reasoning-based stages.

Reinforcement Learning with Verifiable Rewards (RLVR). Following SFT, the model π_{sft} is further refined using RL algorithms—such as PPO (Schulman et al., 2017) or GRPO (Shao et al., 2024b)—to maximize an objective $J_{\text{RL}}(\theta)$ based on a reward $R(x, y)$:

$$J_{\text{RL}}(\theta) = \mathbb{E}_{x \sim \mathcal{D}, y \sim \pi_{\theta}} \left[R(x, y) - \frac{1}{\eta} D_{\text{KL}}(\pi_{\theta} | \pi_{\text{sft}}) \right] \quad (2)$$

where $\eta > 0$ is the inverse temperature parameter governing the strength of the Kullback–Leibler (KL) regularization. This penalty ensures the optimized model π_{θ} does not deviate excessively from the initial π_{sft} . This stage is critical for incentivizing advanced reasoning capabilities in LLMs, aiming to achieve superior performance that transcends the inherent limitations of static SFT datasets.

3.2 The Idealized Post-Training Objective

A critical limitation of the prevailing post-training paradigm (i.e. SFT followed by RL) is that these two stages are predominantly treated as disjoint optimization tasks. While recent studies have attempted to bridge this gap by coordinating training data or scheduling steps (Vattikonda et al., 2025; Kang et al., 2025; Ma et al., 2025), the underlying objective functions remain fundamentally uncoupled. We hypothesize that for post-training to

reach its full potential, SFT should not be viewed merely as a preliminary task, but as an explicit initialization phase mathematically aligned with the subsequent RL objective. By reconciling these stages, we aim to converge toward a singular, comprehensive goal: an **idealized global objective** for post-training.

We formulate this post-training objective as identifying a theoretical target policy π_{global}^* that maximizes expected rewards while remaining anchored to the foundational knowledge of the base model π_{base} . Formally, this global objective is defined as:

$$\begin{aligned} \pi_{\text{global}}^*(\cdot | x) &= \arg \max_{\pi} \mathbb{E}_{x \sim \mathcal{D}, y \sim \pi(\cdot | x)} [\\ &R(x, y) - \frac{1}{\eta} D_{\text{KL}}(\pi(\cdot | x) \| \pi_{\text{base}}(\cdot | x))]. \end{aligned} \quad (3)$$

Following the derivation principles of previous work (Rafailov et al., 2024; Peters et al., 2010), the closed-form solution to Eq. 3 is given by the Gibbs distribution:

$$\pi_{\text{global}}^*(y | x) = \frac{1}{Z_{\text{base}}(x)} \pi_{\text{base}}(y | x) e^{\eta R(x, y)} \quad (4)$$

where $Z_{\text{base}}(x) = \sum_y \pi_{\text{base}}(y | x) e^{\eta R(x, y)}$ is the partition function. This distribution represents the information-theoretically principled balance between maximizing external rewards and preserving the structural priors of the base model. While one could theoretically attempt to optimize π_{base} toward π_{global}^* directly via RL, this approach is computationally intractable for LLMs. In practice, direct sampling during RL often yields vanishingly sparse rewards, which prevents the optimization process from converging.

3.3 Deriving the Principled Initial Policy

To ensure the two-stage post-training process aligns with the idealized global objective, the convergence point of the RL stage must coincide with π_{global}^* . Typically, an RL stage initialized from a policy π_{sft} converges to:

$$\pi_{\text{stage2}}^*(y | x) = \frac{1}{Z_{\text{sft}}(x)} \pi_{\text{sft}}(y | x) \cdot e^{\lambda R(x, y)}, \quad (5)$$

where $\lambda > 0$ governs the strength of the KL regularization. By enforcing the condition $\pi_{\text{stage2}}^* \equiv \pi_{\text{global}}^*$ and substituting Eq. 4 and Eq. 5, we obtain:

$$\frac{\pi_{\text{sft}}(y | x) \cdot e^{\lambda R(x, y)}}{Z_{\text{sft}}(x)} = \frac{\pi_{\text{base}}(y | x) \cdot e^{\eta R(x, y)}}{Z_{\text{base}}(x)} \quad (6)$$

Algorithm 1 GIFT: Gibbs Initialization with Finite Temperature

- 1: **Input:** Dataset \mathcal{D} , Initialized model π_θ , Base model π_{base}
- 2: **Hyper:** Inverse temperature gain β , Learning rate α
- 3: **Initialize:** $\theta \leftarrow \theta_{\text{base}}$
- 4: **while** not converged **do**
- 5: Sample a batch of sequences $(x, y^*) \sim \mathcal{D}$
- 6: Forward pass with base model to get logits z_{base} for all steps t .
- 7: Compute log-probabilities: $\log p_{\text{ref}}(v|x, y_{<t}^*) = \text{LogSoftmax}(z_{\text{base}})_v$
- 8: For each timestep t , construct the advantage-adjusted target logits \hat{z} :

$$\hat{z}_{t,k} = \begin{cases} \log p_{\text{ref}}(k|x, y_{<t}^*) + \beta & \text{if } k = y_t^* \\ \log p_{\text{ref}}(k|x, y_{<t}^*) & \text{if } k \neq y_t^* \end{cases}$$

- 9: Compute target distribution: $\pi_{\text{sft}}^*(\cdot | x, y_{<t}^*) = \text{Softmax}(\hat{z}_t)$
- 10: Update θ by minimizing the cross-entropy loss against soft targets:

$$\mathcal{L}(\theta) = -\frac{1}{B} \sum_{i=1}^B \sum_{t=1}^{|y^*|} \sum_{v \in \mathcal{V}} \pi_{\text{sft}}^*(v | x, y_{<t}^*) \log \pi_\theta(v | x, y_{<t}^*)$$

- 11: $\theta \leftarrow \theta - \alpha \nabla_\theta \mathcal{L}(\theta)$
 - 12: **end while**
 - 13: **return** θ
-

Solving for π_{sft} , we derive the principled initial policy for the subsequent RL stage:

$$\pi_{\text{sft}}^*(y|x) = \frac{1}{Z(x)} \pi_{\text{base}}(y|x) \cdot e^{\beta R(x,y)}, \quad (7)$$

where $\beta = \eta - \lambda$ represents finite inverse temperature for this Gibbs distribution, which serves as a decoupled hyperparameter in practice to accommodate dynamic KL controls during RL. This result provides a thermodynamic critique of current paradigms: standard SFT effectively assumes $\beta \rightarrow \infty$ (a zero-temperature limit), forcing the policy to collapse onto a Dirac distribution. In contrast, GIFT maintains a finite β , acting as a reward-weighted scaling that amplifies high-quality sequences while preserving the structural priors of the base model, thereby maintaining the exploration capacity essential for the subsequent RL. In practice, this target distribution is implemented with autoregressive language models through a token-level approximation, which is provided in Appendix B.

3.4 Proposed Algorithm: GIFT

We minimize the KL divergence between our principled target distribution π_{sft}^* and the parameterized model π_θ . Since the entropy of the target distribu-

tion is constant with respect to θ , this is mathematically equivalent to minimizing the cross-entropy loss, obtaining the following optimization objective:

$$\mathcal{L}(\theta) = -\mathbb{E}_{(x,y^*) \sim \mathcal{D}} \left[\sum_{t=1}^{|y^*|} \sum_{y_t \in \mathcal{V}} \pi_{\text{sft}}^*(y_t|x, y_{<t}^*) \log \pi_\theta(y_t|x, y_{<t}^*) \right] \quad (8)$$

GIFT ensures that while the model is incentivized to prioritize the expert trajectory, it retains the structural knowledge and capabilities of the base model. By preventing premature policy collapse, this approach maintains the exploration capacity essential for the subsequent RL phase. The complete procedure is detailed in Algorithm 1.

4 Experiments

4.1 Experimental setup

Datasets. We utilize **DeepMath-103k** (He et al., 2025), a large-scale mathematical dataset specifically curated for high-difficulty reasoning tasks. It undergoes a rigorous decontamination process against multiple public benchmarks and provides verifiable ground-truth answers to facilitate rule-based rewards. Each problem is accompanied

by high-quality solutions generated by DeepSeek-R1 (DeepSeek-AI et al., 2025a). From the full DeepMath-103k corpus, we randomly sample three disjoint subsets for our experiments: 10,000 samples for SFT, 10,000 samples for RL, and 1,000 samples as a validation set to monitor convergence during the SFT stage.

Evaluation. To comprehensively assess the reasoning capabilities, we employ a suite of 6 widely adopted benchmarks: mathematical reasoning benchmarks **GSM8K** (Cobbe et al., 2021) for grade-school math; **Math500** (Hendrycks et al., 2021), a rigorous subset of the MATH dataset; **AIME24 & AIME25** to test performance on high-difficulty mathematics competitions; and **HumanEval-plus**, **MBPP-plus** (Liu et al., 2023) for code reasoning. Furthermore, to verify generalizability, we evaluate on 4 OOD benchmarks: **GPQA** (Rein et al., 2023) for graduate-level reasoning, **MMLU-Pro** (Wang et al., 2024) and **MMLU-Redux** (Gema et al., 2025) for massive multitask language understanding, **ARC-Challenge** (Clark et al., 2018) for common-sense reasoning. We also validate GIFT on open-ended generation tasks (**MT-Bench** (Bai et al., 2024)), see Appendix D. All evaluations are conducted by VeRL (Sheng et al., 2024) with the vLLM backend. We set the maximum response length to 8,192 tokens and temperature $T = 0.6$ to evaluate the robustness of the policy. For AIME24/25 on Llama-3.1-8B, we report pass@32 instead of pass@1 due to the insufficient discrimination, while maintaining pass@1 for all other benchmarks to ensure consistent evaluation.

Baselines and Implementation. We evaluate various initialization strategies on two backbone models, Qwen2.5-7B and Llama-3.1-8B, categorizing baselines into three groups: (1) **Direct SFT/RL**, which includes standard SFT on the base model and applying RL directly without prior fine-tuning; (2) **Unified Paradigms**, featuring recent methods like LUFFY (Yan et al., 2025) and ReLIFT (Ma et al., 2025); and (3) **SFT-then-RL**, where we compare our proposed GIFT against Standard SFT and several initialization variants. Crucially, to rigorously prove that our gains stem from the reward-calibrated Gibbs re-weighting rather than indiscriminate soft-labeling or task-agnostic base-model mimicking, we include SFT+Entropy (entropy regularization), SFT+Label Smoothing (Soft labeling), and SFT+KD (KL divergence distillation with the base model) as explicit ablations. We also compare with recent SFT methods including DFT (Wu et al.,

2025), ASFT (Zhu et al., 2025a), and PSFT (Zhu et al., 2025b). Notably, we omit the results of Unified Paradigms on Llama-3.1-8B due to their consistently poor performance on this weaker backbone. In the subsequent RL stage, we uniformly employ GRPO (Shao et al., 2024a) via the VeRL framework. Training is configured with a group size of $G = 8$, a learning rate of 1×10^{-6} , a PPO clip ratio of 0.2, and a maximum length of 8,192 tokens for long chain-of-thought reasoning. All models are trained for one epoch on $8 \times$ NVIDIA H200 GPUs. Detailed hyperparameters and settings are provided in Appendix E.

4.2 Main Results

We demonstrate the excellent performance of GIFT initialization from three aspects: significant improvements in reasoning tasks, robust OOD generalization, and superior exploration potential as evidenced by pass@k scaling prior to the RL training.

Reasoning Performance. As shown in Table 1, GIFT consistently achieves best performance across all initialization strategies on both Qwen2.5-7B and Llama-3.1-8B. On Qwen2.5-7B, GIFT attains an average pass@1 of 59.55% (4.49% over SFT), surpassing not only strong SFT variants like PSFT (56.33%) but also complex unified paradigms such as LUFFY (56.69%). Notably, on the challenging AIME benchmark, GIFT yields a substantial gain of nearly 10% over Standard SFT (13.33% \rightarrow 23.33%). On the weaker Llama-3.1-8B, GIFT similarly leads with an impressive 42.96%, outperforming Standard SFT (37.46%) and PSFT (37.70%) by significant margins. In contrast, while simple regularization via SFT + Entropy yields moderate improvements, baselines such as DFT and ASFT exhibit severe degradation. Notably, heuristic approaches like Label Smoothing and KD indiscriminately dilute the supervised signal, leading to performance decay. This demonstrates that GIFT’s effectiveness stems not from simple target softening, but from its reward-calibrated anchor that explicitly boosts the oracle token while preserving the base model’s relative probability mass.

Generalization Capabilities. Table 2 details the OOD performance across different initialization strategies. GIFT demonstrates robust generalization capabilities, effectively mitigating the catastrophic forgetting of general knowledge typically induced by the rigid zero-temperature collapse of Standard SFT and other variants. On Qwen2.5-7B,

Table 1: Average performance of different initialization strategies for subsequent RL on six reasoning benchmarks. The best performance of each strategy across benchmarks is bold.

Method Class	Strategy	GSM8K	AIME24	AIME25	MATH500	HE ⁺	MBPP ⁺	Average
<i>Qwen2.5-7B</i>								
<i>Direct SFT/RL</i>	Direct SFT	90.25	15.00	16.66	74.30	73.20	61.90	55.22
	Direct RL	90.50	12.22	6.67	77.13	73.20	63.80	53.92
<i>Unified Paradigms</i>	LUFFY	92.70	15.00	15.83	80.20	73.20	63.20	56.69
	ReLIFT	91.84	14.06	17.50	79.72	72.60	61.90	56.27
<i>SFT-then-RL</i>	SFT	91.79	13.33	14.44	78.67	72.00	60.10	55.06
	SFT + Entropy	90.90	18.33	11.67	79.90	73.80	61.90	56.08
	SFT + Label Smoothing	90.14	13.33	10.00	73.60	72.00	59.00	53.01
	SFT + KD	91.51	10.00	10.00	78.00	73.80	62.40	54.29
	DFT	86.50	6.67	8.89	65.87	73.20	64.30	50.91
	ASFT	90.65	12.22	7.78	74.07	73.80	63.00	53.59
	PSFT	91.94	15.83	16.67	81.33	73.20	59.00	56.33
	GIFT	92.06	23.33	17.78	82.00	76.20	65.90	59.55
<i>Llama3.1-8B</i>								
<i>Direct SFT/RL</i>	Direct SFT	75.59	6.67	10.00	39.50	39.00	43.10	35.64
	Direct RL	49.18	10.00	16.67	22.27	34.10	48.70	30.15
<i>SFT-then-RL</i>	SFT	73.39	16.67	6.67	39.20	43.30	45.50	37.46
	SFT + Entropy	70.24	23.33	13.33	36.30	40.90	48.40	38.75
	SFT + Label Smoothing	67.90	0.00	0.00	33.40	36.60	47.10	30.83
	SFT + KD	59.28	3.33	0.00	25.00	37.80	49.50	29.15
	DFT	64.75	13.33	3.33	29.47	40.90	49.50	33.55
	ASFT	60.78	13.33	3.33	24.33	39.60	47.10	31.41
	PSFT	74.53	16.67	6.67	39.40	44.50	44.40	37.70
	GIFT	81.33	23.33	13.33	44.45	44.50	50.80	42.96

GIFT achieves an average score of 64.10%, significantly outperforming Standard SFT (59.78%) and maintaining performance parity with complex Unified Paradigms like ReLIFT (64.55%). On Llama-3.1-8B, GIFT secures the highest average performance (55.24%), surpassing all baselines. These results confirm that by maintaining a finite temperature, GIFT successfully retains the structural priors essential for broad generalization, whereas standard zero-temperature SFT is prone to overfitting.

Exploration Potential. We evaluate the exploration capability of the initialized policies by comparing pass@k performance ($k \in \{1, 2, 4, 8\}$) on mathematical reasoning benchmarks prior to RL. As shown in Table 3, GIFT demonstrates superior scaling with sample size compared to Standard SFT. While standard SFT exhibits competitive pass@1 performance (e.g., 39.79% vs. 38.92% on Qwen2.5-7B), its gains diminish as k increases, indicating potential mode collapse. In contrast, GIFT’s advantage expands significantly at higher k ; notably, on Qwen2.5-7B, GIFT reverses the initial gap to achieve a substantial +3.8% lead at pass@8 (62.81% vs. 59.01%). This trend confirms that GIFT preserves a more diverse output distribution, providing a broader and more effective search

space for subsequent reinforcement learning.

4.3 Analysis of Inverse Temperature

The inverse temperature β regulates the fundamental trade-off between exploiting expert data and preserving the exploratory priors of the base model. By varying β , we analyze the sensitivity of post-RL performance to the initialization temperature and directly correlate it with the models’ SFT validation loss dynamics per epoch (Figure 1).

For both models, performance reaches an optimal peak at a finite β before degrading toward the standard SFT baseline ($\beta \rightarrow \infty$). This trend confirms that standard SFT forces a zero-temperature distribution collapse, severely inhibiting the generation diversity required for RL exploration. Crucially, GIFT reveals that the optimal β window is intrinsically tied to the backbone’s resilience to supervision pressure. As illustrated in Figure 1(a) and (c), Llama-3.1-8B exhibits overfitting early in the SFT stage, indicating relatively fragile reasoning priors. Consequently, it enters the “Collapse Zone” much earlier and strictly requires a lower inverse temperature ($\beta \approx 10$) to soften the target distribution and protect its exploration space. Conversely, Qwen2.5-7B maintains a highly stable validation loss (Figure 1(b)), demonstrating robust

Table 2: Average performance of different initialization strategies for subsequent RL on four out-of-distribution benchmarks. The best performance of each strategy across benchmarks is bold.

Method Class	Strategy	GPQA	MMLU-Redux	ARC-Challenge	MMLU-Pro	Average
<i>Qwen2.5-7B</i>						
<i>Direct SFT/RL</i>	Direct SFT	19.70	69.03	82.68	50.23	55.41
	Direct RL	32.32	70.50	73.85	54.33	57.75
<i>Unified Paradigms</i>	LUFFY	34.85	73.30	89.85	59.08	64.27
	ReLIFT	37.88	73.67	89.85	56.82	64.55
<i>SFT-then-RL</i>	SFT	27.78	71.13	85.54	54.67	59.78
	SFT + Entropy	33.33	72.20	87.29	55.60	62.11
	DFT	17.17	57.77	84.85	39.75	49.89
	ASFT	25.25	68.27	86.90	49.98	57.60
	PSFT	34.34	73.79	87.77	59.05	63.74
	GIFT	39.09	73.27	88.01	56.01	64.10
<i>Llama3.1-8B</i>						
<i>Direct SFT/RL</i>	Direct SFT	21.21	61.50	77.82	40.05	50.14
	Direct RL	23.74	52.13	64.59	29.65	42.53
<i>SFT-then-RL</i>	SFT	23.74	55.97	74.49	33.67	46.97
	SFT + Entropy	27.78	63.37	80.25	41.87	53.32
	DFT	24.24	54.27	71.46	35.59	46.39
	ASFT	13.13	47.23	66.42	29.40	39.05
	PSFT	12.12	44.67	46.54	30.14	33.37
	GIFT	30.81	63.17	82.94	44.05	55.24

Table 3: Pass@ k performance (%) prior to RL.

Model	Strategy	$k = 1$	$k = 2$	$k = 4$	$k = 8$
Llama-3.1-8B	SFT	19.06	30.88	36.09	40.49
	GIFT	19.78	31.07	36.79	42.16
Qwen2.5-7B	SFT	39.79	51.33	55.92	59.01
	GIFT	38.92	52.61	57.76	62.81

structural priors. This structural resilience allows Qwen to tolerate and fully benefit from a higher inverse temperature ($\beta \approx 20$), extracting stronger alignment signals before eventually facing capacity collapse (Figure 1(d)). Ultimately, distinct architectures require tailored initialization temperatures, which can be heuristically guided by their varying susceptibilities to overfitting during standard SFT.

4.4 Geometric and Distributional Consistency

To validate whether the finite-temperature initialization fosters a more continuous and stable optimization trajectory during post-training, we analyze the geometric and distributional properties of the model updates. We evaluate the model’s representational and distributional shifts across two sequential stages: **(1)** the transition from the base model to the initialized policy (*Base* \rightarrow *SFT*), and **(2)** the subsequent evolution from the initialized policy to the final RL model (*SFT* \rightarrow *RL*). We quan-

Table 4: Consistency Metrics across Training Stages.

Method	Stage 1 Base \rightarrow SFT			Stage 2 SFT \rightarrow RL		
	Cos \uparrow	L2 \downarrow	KL \downarrow	Cos \uparrow	L2 \downarrow	KL \downarrow
<i>Llama-3.1-8B</i>						
Std. SFT	0.8112	87.33	0.5893	0.9310	53.85	0.2316
GIFT	0.8207	85.05	0.5909	0.9422	49.08	0.2010
<i>Qwen2.5-7B</i>						
Std. SFT	0.9201	117.18	0.3995	0.9764	62.61	0.0426
GIFT	0.9253	113.95	0.3907	0.9869	47.34	0.0327

tify geometric consistency using cosine similarity and L2 distance of the last transformer layer, while measuring distributional consistency via KL divergence and Top- K token overlap (estimated on the held-out validation subset). While smaller representational shifts are not unconditionally beneficial in post-training, they serve as useful proxy metrics in our context to indicate the preservation of structural priors.

Geometric Consistency. As reported in Table 4, GIFT significantly enhances geometric consistency throughout the post-training process. GIFT consistently exhibits higher cosine similarity and lower L2 distance compared to standard SFT across stages and models. This indicates that GIFT effectively absorbs task-specific supervision while adhering to the base model’s semantic manifold, reducing the destructive parameter updates caused

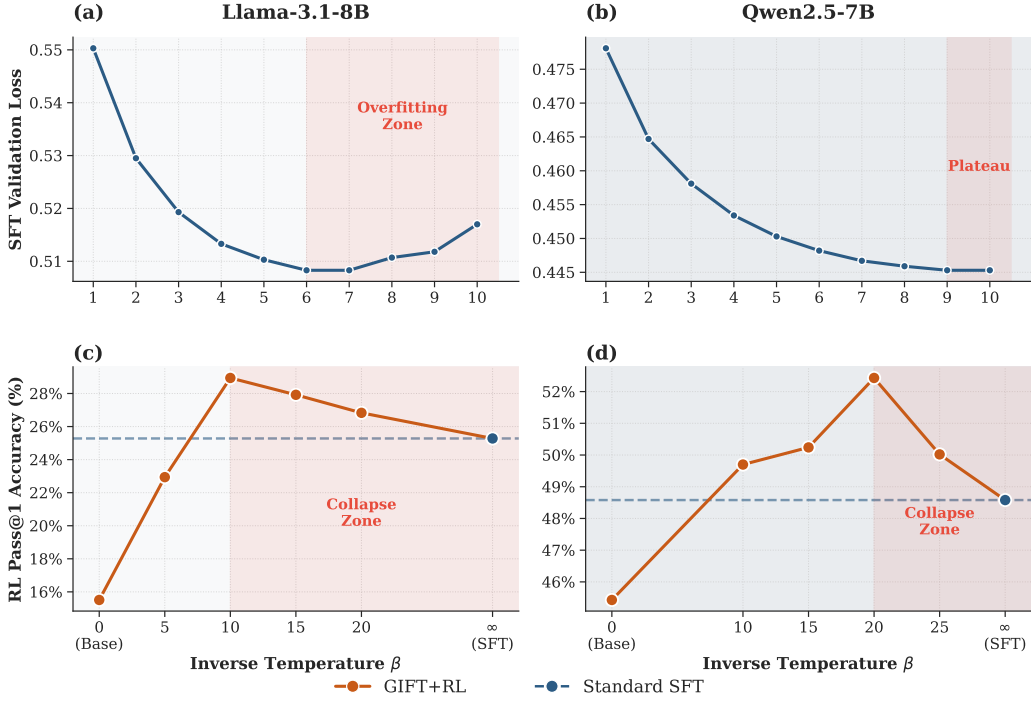


Figure 1: **Correlation between SFT validation dynamics and optimal RL initialization.** (a) and (b) show the SFT validation loss per epoch for Llama-3.1-8B and Qwen2.5-7B, respectively. (c) and (d) illustrate their corresponding post-RL pass@1 accuracy on mathematical reasoning benchmarks across different inverse temperatures β .

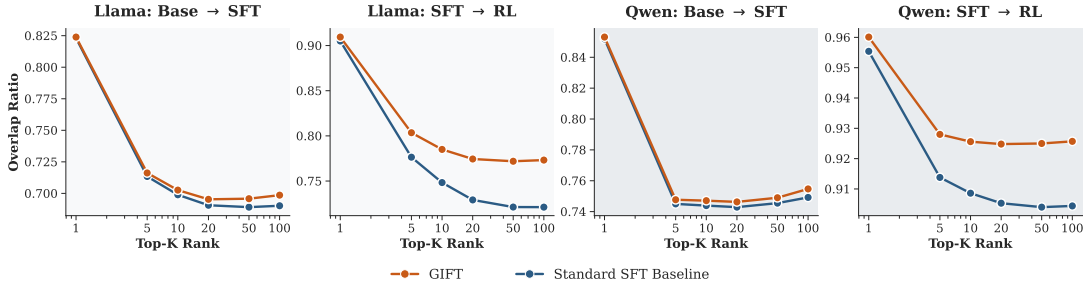


Figure 2: **Top-K Token Overlap Analysis.** Results for Llama-3.1-8B (Left) and Qwen2.5-7B (Right). GIFT exhibits consistently higher token overlap than the SFT baseline.

by standard SFT, thereby providing a more efficient exploration for the subsequent RL stage.

Distributional Consistency. As shown in Table 4, GIFT reduces KL divergence across the entire post-training pipeline in most cases. Complementing this, the top- k token overlap analysis in Figure 2 reveals that GIFT mitigates the drastic distributional shifts characteristic of standard SFT. Moreover, we can observe that the preservation of base priors during SFT stage is effectively leveraged in the subsequent RL stage, manifesting as higher top- k overlap that facilitates more efficient exploration. These proxy metrics suggest that GIFT mitigates drastic distributional shifts, maintaining optimization coherence without forcing a rigid collapse.

5 Conclusion

In this work, we identify the zero-temperature distributional collapse induced by standard SFT and propose Gibbs Initialization with Finite Temperature (GIFT) as a principled initialization for subsequent RL. Experiments validate its effectiveness across reasoning and out-of-distribution tasks, demonstrating well-preserved geometric and distributional consistency throughout post-training. By reconciling the traditional two-stage paradigm, our work offers a theoretically motivated pathway toward constructing robust and generalizable reasoning systems.

6 Limitations

While our framework demonstrates strong performance on models such as Llama-3.1-8B and Qwen2.5-7B, evaluating its scaling properties on massive-scale LLMs is currently constrained by substantial computational requirements. Furthermore, our empirical validation primarily focuses on standard benchmarks within specific linguistic boundaries. Extending this policy optimization approach to highly specialized domains or comprehensive multilingual settings remains a natural avenue for future work.

References

- Ge Bai, Jie Liu, Xingyuan Bu, Yancheng He, Jiaheng Liu, Zhanhui Zhou, Zhuoran Lin, Wenbo Su, Tiezheng Ge, Bo Zheng, and Wanli Ouyang. 2024. [Mt-bench-101: A fine-grained benchmark for evaluating large language models in multi-turn dialogues](#). In *Proceedings of the 62nd Annual Meeting of the Association for Computational Linguistics (Volume 1: Long Papers)*, page 7421–7454. Association for Computational Linguistics.
- Howard Chen, Noam Razin, Karthik Narasimhan, and Danqi Chen. 2025a. [Retaining by doing: The role of on-policy data in mitigating forgetting](#). *Preprint*, arXiv:2510.18874.
- Huayu Chen, Kaiwen Zheng, Qinsheng Zhang, Ganqu Cui, Yin Cui, Haotian Ye, Tsung-Yi Lin, Ming-Yu Liu, Jun Zhu, and Haoxiang Wang. 2025b. [Bridging supervised learning and reinforcement learning in math reasoning](#). *Preprint*, arXiv:2505.18116.
- Jack Chen, Fazhong Liu, Naruto Liu, Yuhan Luo, Erqu Qin, Harry Zheng, Tian Dong, Haojin Zhu, Yan Meng, and Xiao Wang. 2025c. [Step-wise adaptive integration of supervised fine-tuning and reinforcement learning for task-specific llms](#). *Preprint*, arXiv:2505.13026.
- Hyung Won Chung, Le Hou, Shayne Longpre, Barret Zoph, Yi Tay, William Fedus, Yunxuan Li, Xuezhi Wang, Mostafa Dehghani, Siddhartha Brahma, Albert Webson, Shixiang Shane Gu, Zhuyun Dai, Mirac Suzgun, Xinyun Chen, Aakanksha Chowdhery, Alex Castro-Ros, Marie Pellat, Kevin Robinson, and 16 others. 2022. [Scaling instruction-finetuned language models](#). *Preprint*, arXiv:2210.11416.
- Peter Clark, Isaac Cowhey, Oren Etzioni, Tushar Khot, Ashish Sabharwal, Carissa Schoenick, and Oyvind Tafjord. 2018. [Think you have solved question answering? try arc, the ai2 reasoning challenge](#). *Preprint*, arXiv:1803.05457.
- Karl Cobbe, Vineet Kosaraju, Mohammad Bavarian, Mark Chen, Heewoo Jun, Lukasz Kaiser, Matthias Plappert, Jerry Tworek, Jacob Hilton, Reiichiro Nakano, Christopher Hesse, and John Schulman. 2021. [Training verifiers to solve math word problems](#). *Preprint*, arXiv:2110.14168.
- DeepSeek-AI, Daya Guo, Dejian Yang, Haowei Zhang, Junxiao Song, Ruoyu Zhang, Runxin Xu, Qihao Zhu, Shirong Ma, Peiyi Wang, Xiao Bi, Xiaokang Zhang, Xingkai Yu, Yu Wu, Z. F. Wu, Zhibin Gou, Zhihong Shao, Zhuoshu Li, Ziyi Gao, and 181 others. 2025a. [Deepseek-r1: Incentivizing reasoning capability in llms via reinforcement learning](#). *Preprint*, arXiv:2501.12948.
- DeepSeek-AI, Aixin Liu, Bei Feng, Bing Xue, Bingxuan Wang, Bochao Wu, Chengda Lu, Chenggang Zhao, Chengqi Deng, Chenyu Zhang, Chong Ruan, Damai Dai, Daya Guo, Dejian Yang, Deli Chen, Dongjie Ji, Erhang Li, Fangyun Lin, Fucong Dai, and 181 others. 2025b. [Deepseek-v3 technical report](#). *Preprint*, arXiv:2412.19437.
- Yuhao Du, Zhuo Li, Pengyu Cheng, Zhihong Chen, Yuejiao Xie, Xiang Wan, and Anningzhe Gao. 2025. [Simplify rlhf as reward-weighted sft: A variational method](#). *Preprint*, arXiv:2502.11026.
- Aryo Pradipta Gema, Joshua Ong Jun Leang, Giwon Hong, Alessio Devoto, Alberto Carlo Maria Mancino, Rohit Saxena, Xuanli He, Yu Zhao, Xiaotang Du, Mohammad Reza Ghasemi Madani, Claire Barale, Robert McHardy, Joshua Harris, Jean Kaddour, Emile van Krieken, and Pasquale Minervini. 2025. [Are we done with mmlu?](#) *Preprint*, arXiv:2406.04127.
- Arnav Gudibande, Eric Wallace, Charlie Snell, Xinyang Geng, Hao Liu, Pieter Abbeel, Sergey Levine, and Dawn Song. 2023. [The false promise of imitating proprietary llms](#). *Preprint*, arXiv:2305.15717.
- Zhiwei He, Tian Liang, Jiahao Xu, Qiuzhi Liu, Xingyu Chen, Yue Wang, Linfeng Song, Dian Yu, Zhenwen Liang, Wenxuan Wang, and 1 others. 2025. [Deepmath-103k: A large-scale, challenging, decontaminated, and verifiable mathematical dataset for advancing reasoning](#). *arXiv preprint arXiv:2504.11456*.
- Dan Hendrycks, Collin Burns, Saurav Kadavath, Akul Arora, Steven Basart, Eric Tang, Dawn Song, and Jacob Steinhardt. 2021. [Measuring mathematical problem solving with the math dataset](#). *Preprint*, arXiv:2103.03874.
- Ailin Huang, Ang Li, Aobo Kong, Bin Wang, Binxing Jiao, Bo Dong, Bojun Wang, Boyu Chen, Brian Li, Buyun Ma, and 1 others. 2026. [Step 3.5 flash: Open frontier-level intelligence with 11b active parameters](#). *arXiv preprint arXiv:2602.10604*.
- Yuxian Jiang, Yafu Li, Guanxu Chen, Dongrui Liu, Yu Cheng, and Jing Shao. 2025. [Rethinking entropy regularization in large reasoning models](#). *Preprint*, arXiv:2509.25133.
- Feiyang Kang, Michael Kuchnik, Karthik Padthe, Marin Vlastelica, Ruoxi Jia, Carole-Jean Wu, and Newsha

- Ardalani. 2025. [Quagmires in sft-rl post-training: When high sft scores mislead and what to use instead](#). *Preprint*, arXiv:2510.01624.
- Ananya Kumar, Aditi Raghunathan, Robbie Jones, Tengyu Ma, and Percy Liang. 2022. [Fine-tuning can distort pretrained features and underperform out-of-distribution](#). *Preprint*, arXiv:2202.10054.
- Gaotang Li, Ruizhong Qiu, Xiushi Chen, Heng Ji, and Hanghang Tong. 2025. [Beyond log likelihood: Probability-based objectives for supervised fine-tuning across the model capability continuum](#). *Preprint*, arXiv:2510.00526.
- Jiawei Liu, Chunqiu Steven Xia, Yuyao Wang, and Lingming Zhang. 2023. [Is your code generated by chat-GPT really correct? rigorous evaluation of large language models for code generation](#). In *Thirty-seventh Conference on Neural Information Processing Systems*.
- Mingyang Liu, Gabriele Farina, and Asuman Ozdaglar. 2025a. [Uft: Unifying supervised and reinforcement fine-tuning](#). *Preprint*, arXiv:2505.16984.
- Zihan Liu, Zhuolin Yang, Yang Chen, Chankyu Lee, Mohammad Shoeybi, Bryan Catanzaro, and Wei Ping. 2025b. [Acereason-nemotron 1.1: Advancing math and code reasoning through sft and rl synergy](#). *Preprint*, arXiv:2506.13284.
- Lu Ma, Hao Liang, Meiyi Qiang, Lexiang Tang, Xiaochen Ma, Zhen Hao Wong, Junbo Niu, Chengyu Shen, Runming He, Yanhao Li, Bin Cui, and Wentao Zhang. 2025. [Learning what reinforcement learning can't: Interleaved online fine-tuning for hardest questions](#). *Preprint*, arXiv:2506.07527.
- Rui Ming, Haoyuan Wu, Shoubo Hu, Zhuolun He, and Bei Yu. 2025. [One-token rollout: Guiding supervised fine-tuning of llms with policy gradient](#). *Preprint*, arXiv:2509.26313.
- Xueyan Niu, Bo Bai, Wei Han, and Weixi Zhang. 2026. [On the non-decoupling of supervised fine-tuning and reinforcement learning in post-training](#). *Preprint*, arXiv:2601.07389.
- Nvidia, :, Bo Adler, Niket Agarwal, Ashwath Aithal, Dong H. Anh, Pallab Bhattacharya, Annika Brundyn, Jared Casper, Bryan Catanzaro, Sharon Clay, Jonathan Cohen, Sirshak Das, Ayush Dattagupta, Olivier Delalleau, Leon Derczynski, Yi Dong, Daniel Egert, Ellie Evans, and 64 others. 2024. [Nemotron-4 340b technical report](#). *Preprint*, arXiv:2406.11704.
- Long Ouyang, Jeff Wu, Xu Jiang, Diogo Almeida, Carroll L. Wainwright, Pamela Mishkin, Chong Zhang, Sandhini Agarwal, Katarina Slama, Alex Ray, John Schulman, Jacob Hilton, Fraser Kelton, Luke Miller, Maddie Simens, Amanda Askell, Peter Welinder, Paul Christiano, Jan Leike, and Ryan Lowe. 2022. [Training language models to follow instructions with human feedback](#). *Preprint*, arXiv:2203.02155.
- Jan Peters, Katharina Mulling, and Yasemin Altun. 2010. [Relative entropy policy search](#). In *Proceedings of the AAAI Conference on Artificial Intelligence*, volume 24, pages 1607–1612.
- Rafael Rafailov, Archit Sharma, Eric Mitchell, Stefano Ermon, Christopher D. Manning, and Chelsea Finn. 2024. [Direct preference optimization: Your language model is secretly a reward model](#). *Preprint*, arXiv:2305.18290.
- David Rein, Betty Li Hou, Asa Cooper Stickland, Jackson Petty, Richard Yuanzhe Pang, Julien Dirani, Julian Michael, and Samuel R. Bowman. 2023. [Gpqa: A graduate-level google-proof q&a benchmark](#). *Preprint*, arXiv:2311.12022.
- Zhiwen Ruan, Yixia Li, He Zhu, Yun Chen, Peng Li, Yang Liu, and Guanhua Chen. 2025. [Enhancing large language model reasoning via selective critical token fine-tuning](#). *Preprint*, arXiv:2510.10974.
- John Schulman, Filip Wolski, Prafulla Dhariwal, Alec Radford, and Oleg Klimov. 2017. [Proximal policy optimization algorithms](#). *arXiv preprint arXiv:1707.06347*.
- Zhihong Shao, Peiyi Wang, Qihao Zhu, Runxin Xu, Junxiao Song, Xiao Bi, Haowei Zhang, Mingchuan Zhang, Y. K. Li, Y. Wu, and Daya Guo. 2024a. [Deepseekmath: Pushing the limits of mathematical reasoning in open language models](#). *Preprint*, arXiv:2402.03300.
- Zhihong Shao, Peiyi Wang, Qihao Zhu, Runxin Xu, Junxiao Song, Xiao Bi, Haowei Zhang, Mingchuan Zhang, YK Li, Yang Wu, and 1 others. 2024b. [Deepseekmath: Pushing the limits of mathematical reasoning in open language models](#). *arXiv preprint arXiv:2402.03300*.
- Guangming Sheng, Chi Zhang, Zilingfeng Ye, Xibin Wu, Wang Zhang, Ru Zhang, Yanghua Peng, Haibin Lin, and Chuan Wu. 2024. [Hybridflow: A flexible and efficient rlhf framework](#). *arXiv preprint arXiv:2409.19256*.
- Kimi Team, Yifan Bai, Yiping Bao, Guanduo Chen, Jiahao Chen, Ningxin Chen, Ruijue Chen, Yanru Chen, Yuankun Chen, Yutian Chen, and 1 others. 2025. [Kimi k2: Open agentic intelligence](#). *arXiv preprint arXiv:2507.20534*.
- Hugo Touvron, Louis Martin, Kevin Stone, Peter Albert, Amjad Almahairi, Yasmine Babaei, Nikolay Bashlykov, Soumya Batra, Prajjwal Bhargava, Shrutit Bhoale, Dan Bikel, Lukas Blecher, Cristian Canton Ferrer, Moya Chen, Guillem Cucurull, David Esiobu, Jude Fernandes, Jeremy Fu, Wenyin Fu, and 49 others. 2023. [Llama 2: Open foundation and fine-tuned chat models](#). *Preprint*, arXiv:2307.09288.
- Dheeraj Vattikonda, Santhoshi Ravichandran, Emiliano Penalosa, Hadi Nekoei, Megh Thakkar, Thibault Le Sellier de Chezelles, Nicolas Gontier, Miguel Muñoz-Mármol, Sahar Omidi Shayegan, Stefania

- Raimondo, Xue Liu, Alexandre Drouin, Laurent Charlin, Alexandre Piché, Alexandre Lacoste, and Massimo Caccia. 2025. [How to train your llm web agent: A statistical diagnosis](#). *Preprint*, arXiv:2507.04103.
- Shenzhi Wang, Le Yu, Chang Gao, Chujie Zheng, Shixuan Liu, Rui Lu, Kai Dang, Xionghui Chen, Jianxin Yang, Zhenru Zhang, Yuqiong Liu, An Yang, Andrew Zhao, Yang Yue, Shiji Song, Bowen Yu, Gao Huang, and Junyang Lin. 2025. [Beyond the 80/20 rule: High-entropy minority tokens drive effective reinforcement learning for llm reasoning](#). *Preprint*, arXiv:2506.01939.
- Yubo Wang, Xueguang Ma, Ge Zhang, Yuansheng Ni, Abhranil Chandra, Shiguang Guo, Weiming Ren, Aaran Arulraj, Xuan He, Ziyang Jiang, Tianle Li, Max Ku, Kai Wang, Alex Zhuang, Rongqi Fan, Xiang Yue, and Wenhua Chen. 2024. [Mmlu-pro: A more robust and challenging multi-task language understanding benchmark](#). *Preprint*, arXiv:2406.01574.
- Yongliang Wu, Yizhou Zhou, Zhou Ziheng, Yingzhe Peng, Xinyu Ye, Xinting Hu, Wenbo Zhu, Lu Qi, Ming-Hsuan Yang, and Xu Yang. 2025. [On the generalization of sft: A reinforcement learning perspective with reward rectification](#). *Preprint*, arXiv:2508.05629.
- Jianhao Yan, Yafu Li, Zican Hu, Zhi Wang, Ganqu Cui, Xiaoye Qu, Yu Cheng, and Yue Zhang. 2025. [Learning to reason under off-policy guidance](#). *Preprint*, arXiv:2504.14945.
- An Yang, Anfeng Li, Baosong Yang, Beichen Zhang, Binyuan Hui, Bo Zheng, Bowen Yu, Chang Gao, Chengen Huang, Chenxu Lv, Chujie Zheng, Dayiheng Liu, Fan Zhou, Fei Huang, Feng Hu, Hao Ge, Haoran Wei, Huan Lin, Jialong Tang, and 41 others. 2025. [Qwen3 technical report](#). *Preprint*, arXiv:2505.09388.
- Qiyang Yu, Zheng Zhang, Ruofei Zhu, Yufeng Yuan, Xiaochen Zuo, Yu Yue, Weinan Dai, Tiantian Fan, Gaohong Liu, Lingjun Liu, Xin Liu, Haibin Lin, Zhiqi Lin, Bole Ma, Guangming Sheng, Yuxuan Tong, Chi Zhang, Mofan Zhang, Wang Zhang, and 16 others. 2025. [Dapo: An open-source llm reinforcement learning system at scale](#). *Preprint*, arXiv:2503.14476.
- Shiyue Zhang, Shijie Wu, Ozan Irsoy, Steven Lu, Mohit Bansal, Mark Dredze, and David Rosenberg. 2024. [Mixce: Training autoregressive language models by mixing forward and reverse cross-entropies](#). *Preprint*, arXiv:2305.16958.
- Wenhao Zhang, Yuexiang Xie, Yuchang Sun, Yanxi Chen, Guoyin Wang, Yaliang Li, Bolin Ding, and Jingren Zhou. 2025. [On-policy rl meets off-policy experts: Harmonizing supervised fine-tuning and reinforcement learning via dynamic weighting](#). *Preprint*, arXiv:2508.11408.
- He Zhu, Junyou Su, Peng Lai, Ren Ma, Wenjia Zhang, Linyi Yang, and Guanhua Chen. 2025a. [Anchored supervised fine-tuning](#). *Preprint*, arXiv:2509.23753.
- Wenhong Zhu, Ruobing Xie, Rui Wang, Xingwu Sun, Di Wang, and Pengfei Liu. 2025b. [Proximal supervised fine-tuning](#). *Preprint*, arXiv:2508.17784.

A Derivation of the Closed-Form Solution for the Global Objective

In this section, we provide the detailed derivation of the closed-form solution for the optimization problem defined in Eq. 3. We seek to find a policy π that maximizes the following KL-regularized reward objective:

$$J_{\text{RL}}(\theta) = \mathbb{E}_{x \sim \mathcal{D}, y \sim \pi_\theta} \left[R(x, y) - \frac{1}{\eta} D_{\text{KL}}(\pi_\theta \| \pi_{\text{sft}}) \right]$$

Expanding the definition of KL divergence, $D_{\text{KL}}(P \| Q) = \mathbb{E}_{y \sim P} [\log \frac{P(y)}{Q(y)}]$ and using R instead of $R(x, y)$, the objective for a given prompt x can be rewritten as:

$$\begin{aligned} J_{\text{RL}}(\theta) &= \sum_y \pi(y|x) R(x, y) - \frac{1}{\eta} \sum_y \pi(y|x) \log \frac{\pi(y|x)}{\pi_{\text{base}}(y|x)} \\ &= \frac{1}{\eta} \sum_y \pi(y|x) \left[\eta R(x, y) - \log \frac{\pi(y|x)}{\pi_{\text{base}}(y|x)} \right] \\ &= \frac{1}{\eta} \sum_y \pi(y|x) \left[\log \left(\pi_{\text{base}}(y|x) e^{\eta R(x, y)} \right) \right. \\ &\quad \left. - \log \pi(y|x) \right]. \end{aligned} \quad (9)$$

To represent the term inside the logarithm as a valid probability distribution, we introduce the partition function $Z_{\text{base}}(x)$, which acts as a normalization constant:

$$Z_{\text{base}}(x) = \sum_y \pi_{\text{base}}(y|x) e^{\eta R(x, y)}. \quad (10)$$

Substituting this into the objective, we have:

$$\begin{aligned} J_{\text{RL}}(\theta) &= \frac{1}{\eta} \sum_y \pi(y|x) \log \left(\frac{Z_{\text{base}}(x) \pi_{\text{base}}(y|x) e^{\eta R(x, y)}}{\pi(y|x)} \right) \\ &= \frac{1}{\eta} \sum_y \pi(y|x) \left[\log Z_{\text{base}}(x) - \log \frac{\pi(y|x)}{\frac{1}{Z_{\text{base}}(x)} \pi_{\text{base}}(y|x) e^{\eta R(x, y)}} \right]. \end{aligned} \quad (11)$$

Since $\sum_y \pi(y|x) = 1$, the first term simplifies to $\frac{1}{\eta} \log Z_{\text{base}}(x)$. Let $\pi^*(y|x)$ be the Gibbs distribution defined as:

$$\pi^*(y|x) = \frac{1}{Z_{\text{base}}(x)} \pi_{\text{base}}(y|x) e^{\eta R(x, y)}. \quad (12)$$

The objective $J(\pi)$ then becomes:

$$J_{\text{RL}} = \frac{1}{\eta} \log Z_{\text{base}}(x) - \frac{1}{\eta} D_{\text{KL}}(\pi(y|x) \| \pi^*(y|x)). \quad (13)$$

Because the KL divergence is always non-negative ($D_{\text{KL}} \geq 0$) and achieves its minimum value of zero if and only if the two distributions are identical, the objective $J(\pi)$ is maximized when $\pi(y|x) = \pi^*(y|x)$. Thus, the closed-form solution to the post-training global optimum is:

$$\pi_{\text{global}}^*(y|x) = \frac{1}{Z_{\text{base}}(x)} \pi_{\text{base}}(y|x) e^{\eta R(x, y)}. \quad (14)$$

This completes the derivation.

B Derivation of Token-Level Alignment

In this section, we provide the detailed derivation bridging the sequence-level optimal policy $\pi_{\text{sft}}^*(y|x)$ (Eq. 7 in the main text) to the token-level training target $\pi_{\text{sft}}^*(y_t|y_{<t}, x)$ utilized in our algorithm.

Starting from Eq. 7, the optimal sequence-level policy is defined as:

$$\pi_{\text{sft}}^*(y|x) = \frac{1}{Z(x)} \pi_{\text{base}}(y|x) e^{\beta R(x, y)},$$

where $y = (y_1, y_2, \dots, y_T)$. To derive the token-level policy, we aim to find the conditional distribution $\pi_{\text{sft}}^*(y_t|y_{<t}, x)$. According to the definition of conditional probability, we have:

$$\pi_{\text{sft}}^*(y_t|y_{<t}, x) = \frac{\pi_{\text{sft}}^*(y_{\leq t}|x)}{\pi_{\text{sft}}^*(y_{<t}|x)}.$$

To evaluate the marginal probability $\pi_{\text{sft}}^*(y_{\leq t}|x)$, we integrate over all possible future completions $y'_{>t}$:

$$\begin{aligned} \pi_{\text{sft}}^*(y_{\leq t}|x) &= \sum_{y'_{>t}} \pi_{\text{sft}}^*(y_{\leq t}, y'_{>t}|x) \\ &= \frac{1}{Z(x)} \\ &\quad \cdot \sum_{y'_{>t}} \left[\pi_{\text{base}}(y_{\leq t}, y'_{>t}|x) e^{\beta R(x, y_{\leq t}, y'_{>t})} \right] \\ &= \frac{\pi_{\text{base}}(y_{\leq t}|x)}{Z(x)} \\ &\quad \cdot \underbrace{\sum_{y'_{>t}} \pi_{\text{base}}(y'_{>t}|y_{\leq t}, x) e^{\beta R(x, y_{\leq t}, y'_{>t})}}_{\text{Expected exponentiated reward}} \end{aligned} \quad (15)$$

For simplicity, we define the Soft Q-function $Q^*(y_{\leq t})$ as the log-expectation of the exponentiated reward:

$$Q^*(y_{\leq t}) = \log \sum_{y_{>t}} \pi_{\text{base}}(y_{>t}|y_{\leq t}, x) e^{\beta R(x, y)}.$$

This definition allows the marginal probability to be expressed compactly as:

$$\pi_{\text{sft}}^*(y_{\leq t}|x) = \frac{1}{Z(x)} \pi_{\text{base}}(y_{\leq t}|x) e^{Q^*(y_{\leq t})}.$$

Substituting into the conditional probability identity, we obtain:

$$\begin{aligned} \pi_{\text{sft}}^*(y_t|y_{<t}, x) &= \frac{\pi_{\text{sft}}^*(y_{\leq t}|x)}{\pi_{\text{sft}}^*(y_{<t}|x)} \\ &\propto \frac{\pi_{\text{base}}(y_{\leq t}|x) e^{Q^*(y_{\leq t})}}{\pi_{\text{base}}(y_{<t}|x) e^{Q^*(y_{<t})}}. \end{aligned} \quad (16)$$

Using the autoregressive factorization of π_{base} , i.e., $\frac{\pi_{\text{base}}(y_{\leq t}|x)}{\pi_{\text{base}}(y_{<t}|x)} = \pi_{\text{base}}(y_t|y_{<t}, x)$, the optimal token-level policy can be written as:

$$\pi_{\text{sft}}^*(y_t|y_{<t}, x) \propto \pi_{\text{base}}(y_t|y_{<t}, x) \cdot e^{A^*(y_t, y_{<t})}, \quad (17)$$

where $A^*(y_t, y_{<t}) = Q^*(y_{\leq t}) - Q^*(y_{<t})$ denotes the soft advantage function.

While Eq. 17 gives the exact optimal policy, computing A^* is intractable in practice due to the need to sum over all future completions in Q^* . To obtain a tractable approximation, we exploit the sparsity of high-reward trajectories in sequence modeling. The ground-truth trajectory y^* lies in a high-reward region, whereas deviations typically cause $Q^*(y_{\leq t})$ to decay rapidly. This induces a sharply peaked, near-binary advantage landscape: oracle tokens have high values (on the order of β), while off-path tokens have negligible values. Accordingly, we approximate the advantage as β for oracle tokens ($y_t = y_t^*$) and 0 otherwise. Substituting this approximation into Eq. 17 yields the final training target:

$$\pi_{\text{sft}}^*(y_t|y_{<t}, x) \propto \pi_{\text{base}}(y_t|y_{<t}, x) \cdot e^{\beta \cdot \mathbb{1}(y_t=y_t^*)}. \quad (18)$$

C Training Dynamics.

We report the accuracy on mathematical reasoning benchmarks during the RL training in Figure 3. GIFT initialization demonstrates superior sample efficiency and asymptotic performance compared to standard SFT initialization. On Llama-3.1-8B, GIFT maintains a consistent performance advantage over the SFT baseline out the entire optimization process. Meanwhile, on Qwen2.5-7B, we observe a crossover phenomenon: although GIFT begins with slightly lower performance, it rapidly overtakes the SFT baseline within the first 25%

steps. This trajectory indicates that GIFT effectively avoids the premature convergence often induced by rigid supervision, trading off negligible initial exploitation for substantially greater exploration potential and superior long-term gains.

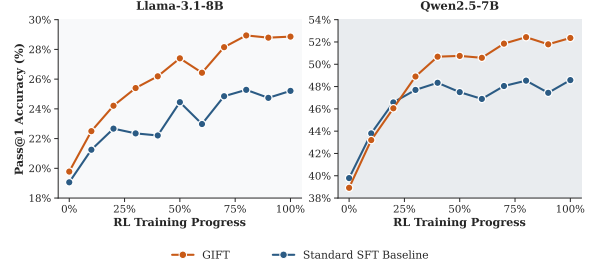


Figure 3: Average pass@1 accuracy across the RL training progress.

D Generalizability on Open-ended Generation Tasks

While our primary evaluation focuses on verifiable mathematics and reasoning, we extend our experiments to the **MT-Bench** benchmark (Bai et al., 2024) to verify whether our token-level approximations maintain generalizability in unconstrained, open-ended conversational settings. As shown in Table 5, GIFT consistently achieves the highest overall scores (*Total*) across both Qwen2.5-7B and Llama-3.1-8B models. Specifically, it excels in categories such as STEM and Extraction, while avoiding the severe performance degradation often observed in standard SFT variants (e.g., SFT+KD or Label Smoothing) when faced with diverse user prompts. These results demonstrate that GIFT successfully preserves the generative priors of the base model, ensuring robust open-ended dialogue capabilities while simultaneously achieving peak reasoning potential.

E Implementation Details

In this section, we provide the detailed experimental configuration to facilitate reproducibility. All experiments are conducted using the VeRL framework (Sheng et al., 2024) on a cluster of $8 \times$ NVIDIA H200 GPUs.

E.1 Supervised Fine-Tuning

Training Configuration. We optimize the base models using the AdamW optimizer with $\beta_1 = 0.9$, $\beta_2 = 0.95$, and a weight decay of 0.01. The global batch size is set to 128. We employ a constant

Table 5: Comprehensive performance on the MT-Bench benchmark across various conversational and reasoning categories.

Strategy	Total	Writing	Roleplay	Reasoning	Math	Coding	Extract	STEM	Humanities
<i>Qwen2.5-7B</i>									
SFT	5.79	4.0	7.7	4.1	5.3	5.3	5.0	6.7	8.2
SFT + Entropy	6.12	4.4	7.7	6.7	4.7	5.0	5.7	7.0	7.8
SFT + Label Smoothing	6.00	4.7	6.6	4.0	6.4	5.2	5.6	6.8	8.7
SFT + KD	6.12	5.5	7.2	4.5	5.8	5.7	5.6	7.1	7.6
DFT	5.60	4.1	5.8	4.0	6.3	5.1	5.8	5.9	7.8
ASFT	5.85	3.7	6.9	4.3	6.1	5.6	5.6	6.5	8.1
PSFT	5.64	3.7	6.7	4.1	4.1	5.7	5.2	7.0	8.6
GIFT	6.34	5.2	6.9	4.8	6.4	5.2	6.5	7.6	8.1
<i>Llama3.1-8B</i>									
SFT	4.46	4.9	5.4	3.5	2.5	3.4	3.8	4.7	7.5
SFT + Entropy	3.94	4.7	4.3	2.8	2.4	2.5	3.7	4.6	6.5
SFT + Label Smoothing	3.99	5.0	4.5	3.0	2.8	2.1	4.5	3.8	6.2
SFT + KD	3.30	2.8	3.3	2.2	4.0	3.3	3.0	4.1	3.7
DFT	5.05	5.0	5.9	3.5	4.2	3.6	5.5	5.6	7.1
ASFT	4.89	5.2	5.6	3.8	3.6	4.4	5.2	4.5	6.8
PSFT	4.19	5.3	4.4	3.0	3.7	2.3	2.7	5.6	6.5
GIFT	5.17	6.4	5.9	4.3	4.1	3.3	4.2	6.0	7.2

learning rate of 1×10^{-5} with no warmup steps. To accommodate long chain-of-thought reasoning, we set the maximum sequence length to 8,192 tokens. Following standard practices for generative fine-tuning, we apply right-side truncation for input sequences. For the explicit SFT ablation variants, we set the regularization coefficient to $\lambda = 0.01$ for both entropy regularization and label smoothing, and apply a distillation weight of $\alpha = 0.1$ for knowledge distillation. For all other baseline methods, we strictly adopt the default hyperparameter settings recommended in their respective original papers to ensure a fair comparison. To initialize the subsequent RL stage, we uniformly select the SFT checkpoint from the 6th epoch across all backbones. As analyzed in Section 4.3 (Figure 1), Llama-3.1-8B reaches its lowest validation loss at this epoch before overfitting. For Qwen2.5-7B, the performance differences after epoch 6 are marginal. Thus, we uniformly adopt the 6th epoch to establish a standardized setting and avoid post-hoc selection bias based on RL downstream dynamics. Finally, to ensure a fair comparison, the direct SFT baseline is trained on a combined dataset comprising both SFT and RL data to match the total data size configuration.

E.2 Reinforcement Learning

Following SFT, we apply the Group Relative Policy Optimization (GRPO) algorithm (Shao et al., 2024b) to refine the policy. During the exploration phase, we sample $G = 8$ outputs per prompt with a temperature of $T = 1.0$ to encourage di-

versity. The policy is optimized using a constant learning rate of 1×10^{-6} and a global batch size of 128 (mini-batch size of 64). We set the clip ratio to 0.2 and disable advantage normalization (norm_adv_by_std=False). To prevent reward hacking, we restrict training to 1 epoch.

E.3 Evaluation and Reward Mechanism

Evaluation. We report the average pass@1 accuracy across four runs for all benchmarks, except for Llama3.1-8b on AIME24/25, where we report pass@32 due to limited model ability. We merge FSDP checkpoints and utilize vLLM for high-throughput inference with a temperature of $T = 0.6$ and a max token limit of 8,192.

Reward Function. We employ a cascaded binary reward function that sequentially utilizes OpenMathInstruct extraction rules and the MathVerify parser. To ensure stability, the verification process is guarded by a 10-second thread-based timeout, assigning a reward of 1.0 if either method validates the solution against the ground truth.

F Use of AI Assistants

We utilized AI assistants exclusively for grammatical polishing and LaTeX formatting assistance.